RGNZ/MGPB

Comparative analysis on the impact of water saturation on the performance of in-situ combustion

Rudarsko-geološko-naftni zbornik
(The Mining-Geology-Petroleum Engineering Bulletin)
UDC: 550.8
DOI: 10.17794/rgn.2022.4.14

Original scientific paper

Tummuri Naga Venkata Pavan[1]; Srinivasa Reddy Devarapu[2]; Suresh Kumar Govindarajan[3]

[1] Research Scholar, Reservoir Simulation Laboratory, Petroleum Engineering Programme, Department of Ocean Engineering, Indian Institute of Technology – Madras, Chennai, India. ORCID: 0000-0003-4649-1442

[2] Assistant Professor, Energy Cluster, School of Engineering, University of Petroleum & Energy Studies, Dehradun. ORCID: 0000-0002-9557-4271

[3] Professor, Reservoir Simulation Laboratory, Petroleum Engineering Programme, Department of Ocean Engineering, Indian Institute of Technology – Madras, Chennai, India. ORCID: 0000-0003-3833-5482

Abstract

The amount of oil together with the water Originally in Place (OIP), makes up the liquid phase in heavy oil reservoir systems. This amount of liquid present in the pores of the reservoir system, known as liquid saturation, plays a vital role in improving oil recovery through the In-Situ Combustion (ISC) process. The oil phase acts as a fuel in generating the thermal energy required for viscosity reduction and the water phase supports in the formation of an enlarged condensation zone that aids in the higher mobility of the low viscous oil. A numerical investigation is carried out to study the role of water saturation on the performance of in-situ combustion in a heavy oil reservoir. A finite-difference based numerical model is developed and validated for water recovery. The model is then used to carry out the impact of liquid saturation on the performance of the ISC, as it plays a vital role in screening criteria for the selection of ISC. The numerical results projected a significant effect on the thermal and production profile during the process. A comparison between the effect of variation in water and oil saturations projected a significant increase in reservoir temperatures with increased water saturation than the oil saturation. The highest reservoir temperatures are observed at the maximum liquid (oil and water together) saturation. Further, the additional water drive provided by increased water saturation is observed to contribute to early production rates.

Keywords:
enhanced oil recovery; thermal; saturation; in-situ combustion; numerical modelling

1. Introduction

Petroleum fossil fuels continue to be the world's primary energy source (**Sanjeet et al., 2022**). With easy to produce reserves explored, the reserve replacement is expected to play a significant role in fulfilling global energy demands. The heavy oil resources that are difficult to produce and the oil remaining in place after secondary recovery processes are the potential target for reserve replacement. Further, two thirds of the global hydrocarbon resources are mainly the extra heavy and heavy crude oil reserves (**Meyer et al., 2007**). Enhanced Oil Recovery (EOR) techniques based on thermal energy application increase the recovery rates of these difficult to produce heavy oil reservoirs by reducing their viscosity by injecting heat or generating heat inside the reservoir (**Bealessio et al., 2021**). In-Situ Combustion (ISC) is a proven efficient and economical TEOR method in which heat is generated inside the reservoir by combustion of a portion of crude oil in place (**Sarathi et al., 1999; Bueno and Mejia, 2022**). In this process, air (or air enriched with oxygen or pure oxygen) is injected into a porous heavy oil reservoir, which reacts with crude oil in a series of chemical reactions forming different zones, as shown in **Figure 1**. The exothermic reactions give off heat. At elevated temperatures, the heavy oil undergoes cracking to produce low molecular weight hydrocarbons and carbon rich solid components. The carbon rich solid is commonly known as coke.

The heat generated in-situ contributes to thermal expansion and distillation processes, ultimately resulting in the viscosity reduction of native crude oil. The carbon rich coke acts as fuel for sustaining the combustion (**Greaves et al., 2000**). The oxides of carbon in the gaseous phase help to decrease density and provide for an additional gas drive promoting increased oil production rates (**Kristensen et al., 2007; Zheng et al., 2017**). Therefore, ISC can be represented as the combination process encompassing some aspects of nearly every oil recovery method such as: distillation, steam displacement, hydrocarbon miscible flooding, immiscible gas

Corresponding author: Tummuri Naga Venkata Pavan
e-mail address: pavantummuri@gmail.com

(N_2) displacement, and water flooding (both hot and cold) (**Ahmed and Meehan, 2012**).

The air injected at the injection well enters the burnt zone burning most of the oil surrounding the injection well. A low temperature at the initial period propagates an unreacted oxygen front, which is unfavourable for combustion (**Xu et al., 2018**). So, the oxygenation of the heavy oil increases the temperature in the reservoir in the burnt zone (**Yuan et al., 2019**). As the thermal front reaches the downstream of the burning zone, an enormous amount of heat energy is released from the combustion of crude oil with air. This results in an increase in reservoir temperature. As the local reservoir temperatures reach a value greater than the saturation temperature of the water, the temperature continues to rise abruptly reaching a maximum value (peak temperature) in the combustion zone. The elevated temperatures cause cracking and vaporisation of heavy oil resulting in the formation of a vaporisation zone. The water produced during combustion reactions and the water present initially in the formation vaporise and mobilize ahead of oil, forming a steam plateau zone. The endothermic nature of the cracking reaction and the mixing of native reservoir oil with combustion products results in a drastic decrease in reservoir temperature to a value less than the saturation temperature of water resulting in water condensation forming a hot water bank. The temperature continues to drop reaching the initial reservoir temperature. The hot water bank then aids in increasing the oil recovery by driving the native oil ahead of it to the production well.

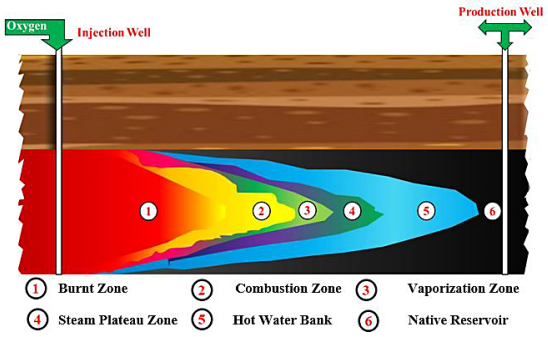

Figure 1: Schematic of the in-situ combustion process in a typical porous reservoir

Researchers have reported the performance of ISC on heavy oil reservoirs (**Wang et al., 2020; He et al., 2022**), on abandoned wells in the absence of CO_2 production (**Han et al., 2021**). However, the inception of ignition plays a vital role in the quantum of heat energy released as well as the mobilization of native reservoir oil, which is proposed to depend on the amount of oil and water present in the reservoir (**Aleksandrov et al., 2015**). Moreover, sustenance of the ignition is dictated by the Critical Ignition Saturation (CIS), the maximum water saturation (**Nestervo et al., 2007**). Further, the inception of the combustion at the interface of the oil-water is reported to improve the oil recovery (**Ado, 2020**). In this context, an attempt has been made to economically understand the effect of water saturation on the performance of the in-situ combustion. Therefore, the specific objective of the present work is to numerically model the in-situ combustion process in a typical heavy oil reservoir and carry out sensitivity studies on the water saturation to quantify its impact on the thermal profiles aiding the viscosity reduction of native reservoir oil and overall oil recoveries.

2. ISC Model

The developed ISC model is compositional in nature. The conservative equations representing conductive and convective heat transport and coupled with mass transfer by convection in a typical porous oil reservoir are as given in the **Equations 1 and 2** (**Suresh and Srinivasa., 2017**). The model considers the pseudo-componentisation of the native crude oil into six components distributed among 4 phases (as shown in **Table 1**), whose equilibrium composition is modelled using a pseudo-K-value approach (**Srinivasareddy and Suresh., 2015**). Mass transfer by diffusion is neglected (**Paceman, 1997**). The reservoir is assumed to be in thermodynamic equilibrium, and the interphase mass transfer is assumed to occur under equilibrium conditions.

$$\frac{\partial}{\partial t}[\phi \Sigma_j S_j \rho_j y_{ij}] = -\nabla.[\Sigma_j \rho_j y_{ij} \upsilon_j] - Q_i + \Sigma_r q_{ir} \quad (1)$$

$$\frac{\partial}{\partial t}[\phi \Sigma_j S_j \rho_j U_j] + \frac{\partial}{\partial t}[C_c U_c + (1-\phi)\rho_f U_f] =$$

$$= \nabla.(\lambda_f \nabla T) - \nabla.[\Sigma_j \rho_j H_j \upsilon_j] - \dot{Q} + \Sigma_r H_r \quad (2)$$

Equation 1 represent an accumulation in terms of saturation S, advection, production rate Q and, sink/source due to reactions, respectively for each component i. The terms on the LHS of the **Equation 2** are thermal energy accumulation in terms of internal energy U in fluid phases j, solid coke phase and formation respectively. The RHS terms represent conduction expressed in terms of thermal conductivity λ, convection, heat energy associated with the production of fluids $\dot{Q}$ and heat energy associated with reactions respectively. Further, the subscripts c and f represent solid coke phase and formation respectively. The Darcy equation is used to calculate the fluid phase velocities υ as given in the **Equation 3**, where μ is viscosity, K_{abs} is absolute permeability, K_r is relative permeability, P is pressure and g is acceleration due to gravity. The sink and source term q of the component i due to reaction r along with heat generation rate H and rate of reaction R are given by **Equations 4 and 5** respectively.

$$\upsilon_j = -\frac{\kappa_{abs}\kappa_{rj}}{\mu_j}[\nabla.P_j - \rho_j g \nabla.Z] \quad (3)$$

$$q_{ir} = S_{ir} R_r \quad (4)$$

$$H_r = \Delta H_r R_r \quad (5)$$

$$R_r = A_r e^{\left(\frac{-E_r}{RT}\right)} \Pi_r C_{jr}^{n_{jr}} \quad (6)$$

Where:

ΔH – enthalpy,
A – Arrhenius constant,
$\acute{R}$ – universal gas constant,
E – activation energy,
T – temperature,
ρ – density,
ϕ – porosity,
C – molar concentration.

Initial and boundary conditions are as shown in the **Equation 7,** where ξ is any primary dependent variable.

$$\xi(t=0, x \geq 0) = \xi_{initial};\ \xi(t>0, x=0) = \xi_{injection}$$
$$\text{and } \xi(t>0, x=L) = \xi_{production} \quad (7)$$

Table 1: Components used in the ISC Model

S.No.	Component	Phase
1	Light oil	Liquid and Gas
2	Heavy oil	Liquid and Gas
3	Water	Liquid and Gas
4	Oxygen	Gas
5	Inert gas	Gas
6	Coke	Solid

Table 2: Reservoir input parameters

Component	Heavy oil	Light Oil	Oxygen	Inert Gas
Molecular Weight	170	44	32	44
Critical Temperature [K]	657.9	369.1	154.8	304.2
Critical Pressure [kPa]	1824.35	4246.48	5033.9	7398..07
Density (**Lin et al., 1984**)	$\rho_{o_i} = \left(a_{1_i} - a_{2_i} T\right)^{\left[a_{3_i}(P-101.325)\right]}$			
a_1	5.356×10^{3}	18.119×10^{3}	-	-
a_2	3.686	25.084	-	-
a_3	6.892×10^{-5}	1.530×10^{-3}	-	-
Viscosity (**Lin et al., 1984**)	$\mu_o = b_{1_o} \exp(b_{2o}/T)$		$\mu_g = b_{1_g}(b_{2g} + b_{3_g} T)$	
b_1	3.376×10^{-17}		1.8×10^{-13}	
b_2	5.824×10^{3}		2.833	
b_3	-		0.792	
Heat Capacity (**Yang and Gates, 2009**)	$C_{P_{i,j}} = C_{P_{j,1}} + C_{P_{j,2}} T + C_{P_{j,3}} T^2 + C_{P_{j,4}} T^3$			
C_{P1}	126	60	28.1	19.8
C_{P1}	0.55	0.131	-3.68×10^{-6}	7.34×10^{-2}
C_{P1}		-	1.75×10^{-5}	5.6×10^{-5}
C_{P1}		-	-1.06×10^{-8}	1.71×10^{-8}

Reaction Kinetic Parameters (Crookston et al., 1979)			
Reaction (r)	A_r	H_r (KJ/gmol)	E_r (KJ/gmol)
Heavy Oil Cracking	3,00,000 kPa/day	46.5	66.99
Heavy Oil Oxidation	1,45,000 kPa/day	8,120	77.46
Light Oil Oxidation	1,45,000 kPa/day	2,210	77.46
Coke Oxidation	1,45,000 kPa/day	523	54.43

Initial Conditions (Srinivasa and Suresh, 2014b)	
Water saturation	0.2
Oil saturation	0.5
Gas saturation	0.3
mole fraction of Heavy oil	1.0
mole fraction of Light oil	0.0
Reservoir Properties (Crookston et al., 1979)	
Porosity	0.38
Absolute Permeability, m^2	$4x10^{-12}$
Reservoir temperature, K	367
Reservoir pressure, KPa	455
Length, m	50

The kinetic model considers four chemical reactions and is adopted from (**Crookston et al., 1979**). The ISC model input values and the reservoir parameters are reported in **Table 2**. All physical properties are allowed to function as dependent variables (**Crookston et al., 1979; Grabowski et al., 1979; Coats, 1980**). Further the parameters a_1, a_2, a_3, b_1, b_2, b_3 used in the equations are constants and C_{Pi} is the heat capacity constant. The model considers capillary pressure, and the heat loss to the surrounding base cap rock is calculated using a semi-analytical approach developed by **Srinivasa and Suresh., 2014a**.

A block centred finite difference based numerical tool is used to solve the model equations. The numerical model considers seven conservation equations ($n_c + 1$) for seven dependent variable sets $\{P_g, T_g, S_o, S_w, x_{ho}, y_{o_2}, C_C\}$. The choice of primary variables is based on numerical analysis experiences in modelling in-situ combustion reported by **Rubin and Vinsome, (1980); Wood, 1990; Suresh and Srinivasa, 2017.** The Forward Euler technique is used to discretise the temporal terms representing the transient storage of primary dependent variables and one point upstream approximation for flux terms to reach a fully implicit state (**Grabowski et al., 1979**). The discretised conservative equations for volatile oil components, water components, non-condensable gas components, coke (solid-phase) and energy balance, respectively, are of the form as shown in the **Equations 8** to **12**, where the transmissibility term τ and the head term ϕ, respectively are expressed by **Equations 13 and 14.**

$$\frac{V}{\Delta t}\left[\left(\varphi^{n+1}\rho_{o_i}^{n+1}s_{o_i}^{n+1}X_{o_i}^{n+1}-\varphi^{n}\rho_{o_i}^{n}s_{o_i}^{n}X_{o_i}^{n}\right)+\left(\varphi^{n+1}\rho_{g_i}^{n+1}s_{g_i}^{n+1}Y_{g_i}^{n+1}-\varphi^{n}\rho_{g_i}^{n}s_{g_i}^{n}Y_{g_i}^{n}\right)\right]= T_{o_i}^{n+1}X_{o_i}^{n+1}\left(\Phi_{o_{i+1}}^{n+1}-\Phi_{o_i}^{n+1}\right)+T_{o_{i-1}}^{n+1}X_{o_{i-1}}^{n+1}\left(\Phi_{o_{i-1}}^{n+1}-\Phi_{o_i}^{n+1}\right)+T_{g_i}^{n+1}Y_{o_i}^{n+1}\left(\Phi_{g_{i+1}}^{n+1}-\Phi_{g_i}^{n+1}\right) + T_{g_{i-1}}^{n+1}Y_{o_{i-1}}^{n+1}\left(\Phi_{g_{i-1}}^{n+1}-\Phi_{g_i}^{n+1}\right)+Q_{o_i}^{n+1}+\Sigma^{s}r_{k_i}^{n+1} \tag{8}$$

$$\frac{V}{\Delta t}\left[\left(\varphi^{n+1}\rho_{w_i}^{n+1}s_{w_i}^{n+1}-\varphi^{n}\rho_{w_i}^{n}s_{w_i}^{n}\right)+\left(\varphi^{n+1}\rho_{g_i}^{n+1}s_{g_i}^{n+1}Y_{w_i}^{n+1}-\varphi^{n}\rho_{g_i}^{n}s_{g_i}^{n}Y_{w_i}^{n}\right)\right]= T_{w_i}^{n+1}\left(\Phi_{w_{i+1}}^{n+1}-\Phi_{w_i}^{n+1}\right)+T_{w_{i-1}}^{n+1}\left(\Phi_{w_{i-1}}^{n+1}-\Phi_{w_i}^{n+1}\right)+T_{g_i}^{n+1}Y_{w_i}^{n+1}\left(\Phi_{g_{i+1}}^{n+1}-\Phi_{g_i}^{n+1}\right) + T_{g_{i-1}}^{n+1}Y_{w_{i-1}}^{n+1}\left(\Phi_{g_{i-1}}^{n+1}-\Phi_{g_i}^{n+1}\right)+Q_{w_i}^{n+1}+\Sigma^{s}r_{k_i}^{n+1} \tag{9}$$

$$\frac{V}{\Delta t}\left(\varphi^{n+1}\rho_{g_i}^{n+1}s_{g_i}^{n+1}Y_{g_i}^{n+1}-\varphi^{n}\rho_{g_i}^{n}s_{g_i}^{n}Y_{g_i}^{n}\right)= T_{g_i}^{n+1}Y_{g_i}^{n+1}\left(\Phi_{g_{i+1}}^{n+1}-\Phi_{g_i}^{n+1}\right)+T_{g_{i-1}}^{n+1}Y_{g_{i-1}}^{n+1}\left(\Phi_{g_{i-1}}^{n+1}-\Phi_{g_i}^{n+1}\right)+Q_{g_i}^{n+1}+\Sigma^{s}r_{k_i}^{n+1} \tag{10}$$

$$\frac{V}{\Delta t}\left(C_{c_i}^{n+1}-C_{c_i}^{n}\right)=\Sigma^{s}r_{k_i}^{n+1} \tag{11}$$

$$\frac{V}{\Delta t}\left(\left(1-\varphi^{n+1}\right)\rho_{r_i}^{n+1}U_{r_i}^{n+1}-\left(1-\varphi^{n}\right)\rho_{r_i}^{n}U_{r_i}^{n}\right)+\left(\varphi^{n+1}\rho_{o_i}^{n+1}s_{o_i}^{n+1}X_{o_i}^{n+1}-\varphi^{n}\rho_{o_i}^{n}s_{o_i}^{n}X_{o_i}^{n}\right) +\left(\varphi^{n+1}\rho_{g_i}^{n+1}s_{g_i}^{n+1}Y_{g_i}^{n+1}-\varphi^{n}\rho_{g_i}^{n}s_{g_i}^{n}Y_{g_i}^{n}\right)+\left(\varphi^{n+1}\rho_{g_i}^{n+1}s_{g_i}^{n+1}Y_{w_i}^{n+1}-\varphi^{n}\rho_{g_i}^{n}s_{g_i}^{n}Y_{w_i}^{n}\right) +\left(\varphi^{n+1}\rho_{c_i}^{n+1}U_{c_i}^{n+1}-\varphi^{n}\rho_{c_i}^{n}U_{c_i}^{n}\right)]=K_{f_i}^{n+1}\left(T_{i+1}^{n+1}-T_i^{n+1}\right)+K_{f_{i-1}}^{n+1}\left(T_{i-1}^{n+1}-T_i^{n+1}\right) +T_{o_i}^{n+1}h_{o_i}^{n+1}\left(\Phi_{o_{i+1}}^{n+1}-\Phi_{o_i}^{n+1}\right)+T_{o_{i-1}}^{n+1}h_{o_{i-1}}^{n+1}\left(\Phi_{o_{i-1}}^{n+1}-\Phi_{o_i}^{n+1}\right)+T_{g_i}^{n+1}h_{g_i}^{n+1}\left(\Phi_{g_{i+1}}^{n+1}-\Phi_{g_i}^{n+1}\right) +T_{g_{i-1}}^{n+1}h_{g_{i-1}}^{n+1}\left(\Phi_{g_{i-1}}^{n+1}-\Phi_{g_i}^{n+1}\right)+T_{w_i}^{n+1}h_{w}^{n+1}\left(\Phi_{w_{i+1}}^{n+1}-\Phi_{w_i}^{n+1}\right)+T_{w_{i-1}}^{n+1}h_{w_{i-1}}^{n+1}\left(\Phi_{w_{i-1}}^{n+1}-\Phi_{w_i}^{n+1}\right) +(Q_{o_i}^{n+1}h_{o_i}^{n+1}+Q_{g_i}^{n+1}h_{g_i}^{n+1}+Q_{w_i}^{n+1}h_{w_i}^{n+1})+\Sigma H_i^{n+1}r_k^{n+1} \tag{12}$$

$$\tau_{jx}=\frac{A_x}{\Delta x}\frac{k_{abs_x}k_{r_j}}{\mu_j}\rho_j \tag{13}$$

$$\Phi_j=P_j-\rho_j g Z_j \tag{14}$$

The equations are coupled and non-linear in primary dependent variables and are solved by a Newton iterative solver, similar to that proposed by (**Rubin and Buchanan, 1985; Srinivasa and Suresh, 2015; Suresh and Srinivasa, 2017**). The discretised conservation equations can be expressed in matrix form, as shown in the **Equation 15**. J in the **Equation 15** represents a Jacobian sub-matrix for each block resulting from conservation equations. It is calculated using the secant method (**Press et al., 1992**) as shown in the **Equation 16.**

$$\begin{bmatrix} J & J & & \cdots & & \cdots & \\ J & J & J & & & & \\ & \vdots & & \ddots & & \vdots & \\ & & & & J & J & J \\ & \vdots & & \cdots & & J & J \end{bmatrix} \begin{bmatrix} \delta_1 \\ \delta_2 \\ \vdots \\ \vdots \\ \delta_n \end{bmatrix} = - \begin{bmatrix} R_1 \\ R_2 \\ \vdots \\ \vdots \\ R_n \end{bmatrix} \quad (15)$$

$$\begin{bmatrix} \frac{\partial F_1}{\partial \delta_1} & \frac{\partial F_1}{\partial \delta_2} & \cdots & \frac{\partial F_1}{\partial \delta_n} \\ \frac{\partial F_2}{\partial \delta_1} & \frac{\partial F_2}{\partial \delta_2} & & \frac{\partial F_2}{\partial \delta_n} \\ \vdots & & \ddots & \vdots \\ \frac{\partial F_n}{\partial \delta_1} & \frac{\partial F_n}{\partial \delta_2} & \cdots & \frac{\partial F_n}{\partial \delta_n} \end{bmatrix} \quad (16)$$

Where:

δ_i – the unknowns,

R_1 – the conservation equation residuals.

To ensure the stability of the solution, the time-step size has to vary with the rates of changes in the primary variables. This approach is commonly known as adaptive time stepping and is unconditionally stable (**Thomas and Gladwell, 1988; Wood, 1990; Kavetski et al., 2001**). Therefore, the time step size at any time level in the present work is automatically calculated by maintaining the maximum changes in primary dependent variables ζ to be less than defined norm η as given in **Equation 17**. The choice of norm η and damping factor ω is made on the basis of numerical analysis experiences reported in ISC modelling (**Grabowski et al., 1979; Srinivasa and Suresh, 2015**). The typical norms of 400 kPa, 40 K and 0.2 respectively for pressure, temperature and saturation are used in the present work.

$$\Delta t^{n+1} = \Delta t^n \left[\frac{(1+\omega)\eta}{\zeta + \omega\eta}\right]_{\min} \quad (17)$$

3. Results and Discussion

Figure 2 compares the cumulative recovery of water obtained from the present numerical model with the dry combustion data reported by **Crookston et al. (1979)**. Cumulative water recovery is the volumetric water recovery expressed as a percentage of the Original Water

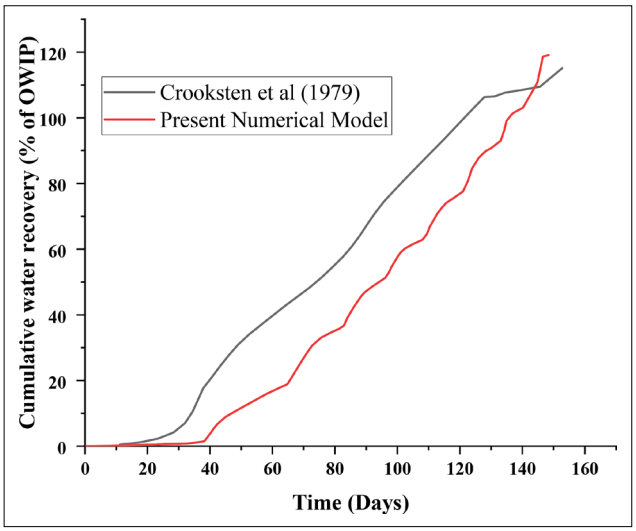

Figure 2: Comparison of water production from the present numerical model with Crooksten et al., 1979

In Place (OWIP). An oil and water saturation of 50% and 20% are maintained for the base case, accounting for the 1.0408×10^3 stock tank m^3 of OWIP. The present numerical model results projected an overall cumulative water recovery of about 117.2%. However, the deviation in the predicted water recovery attributes to the fluid models used in estimating the vapour-liquid equilibrium composition. The cumulative water recovery exceeds 100% because of the water formed in the oxidation reaction. It is critically observed that, out of all the water recovery, 97.3% of water is produced in the liquid phase and 19.9% in the vapour phase.

Figure 3 presents the sensitivity of initial water saturation on the temporal distribution of oil saturation. The numerical results project prolonged saturation profiles with a slight decrease in oil saturation values for increased initial water saturation. This is because an increase in water situation causes an increased amount

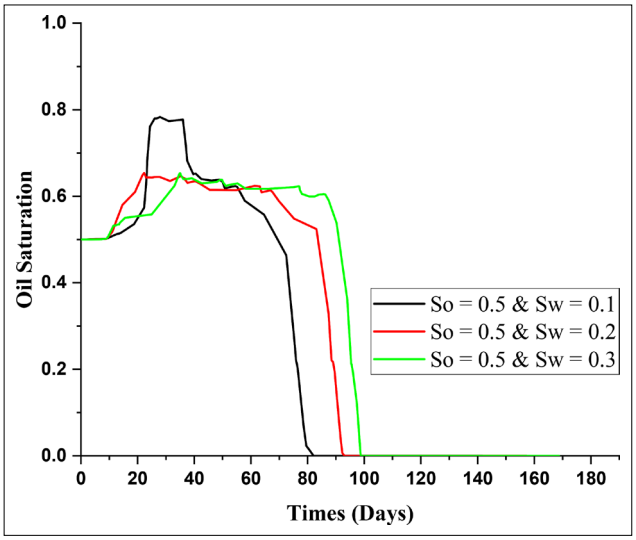

Figure 3: Effect of liquid saturation on oil saturation

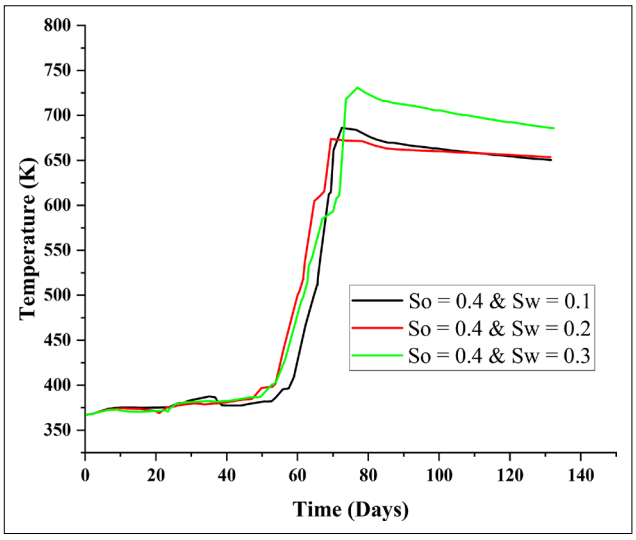

Figure 4: Effect of oil and water saturation on reservoir temperature for So = 0.4

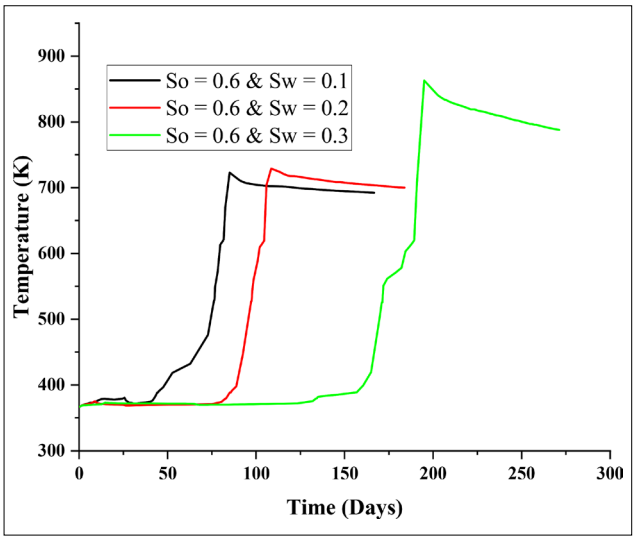

Figure 6: Effect of oil and water saturation on reservoir temperature for So = 0.6

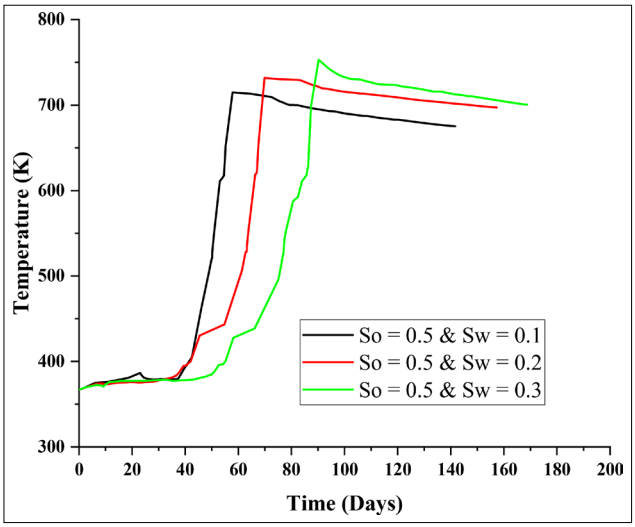

Figure 5: Effect of oil and water saturation on reservoir temperature for So = 0.5

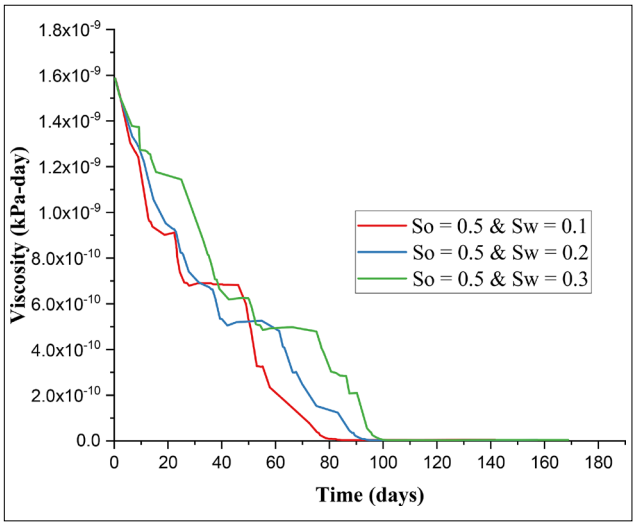

Figure 7: Effect of oil and water saturation on oil viscosity for So = 0.5

of OWIP compared to the Original Oil In Place (OOIP). The elevated temperature profiles associated with the high water content (as seen in **Figures 4**, **5**, and **6**.) cause a reduction in oil viscosities as shown in **Figure 7**, resulting in increasing mobility of the oil phase. The maximum oil saturations attained are observed to decrease by about 20% (87% to 67%) for a decrease in water saturation by 10% (20% to 10%), which indicates a reduction in oil phase blockage reported for an increase in initial oil saturations (**Srinivasa and Suresh, 2014b**). This is further confirmed by a decrease in the time taken (68 days to 55 days) to sweep the oil from a location in a reservoir to the production well.

Further, the initial water saturation is observed to have a pronounced effect on the thermal/temperature profiles, as seen in **Figures 4**, **5**, and **6.** The numerical results projected an increase in reservoir temperature with increased oil and water saturation. Water saturation is found to have a predominant effect on reservoir temperature at higher oil saturations. As seen in **Figure 6,** the change in peak temperature is about 150 K when the water saturation was increased from 20% to 30% for a constant oil saturation of 60%. The numerical results projected that aqueous water present in the reservoir restricts the local temperatures at or below the steam temperature. Once the reservoir pressure exceeds water saturation pressure when the water starts to vaporise, the reservoir temperatures are also found to increase steeply.

An increase in average reservoir temperature by about 20 K and 50 K is observed to increase water saturation from 10% to 20 % and 20% to 30%. However, the average temperatures increased by about 20 K and 140 K for the same amount of increase in water saturation from 10% to 20 % and 20% to 30%, respectively, confirming the ef-

fect of water saturation at high oil saturation conditions. Further, it is critically observed that the rate of increase in reservoir temperature is found to depend strongly on water content (as seen in **Figures 4**, **5**, and **6**).

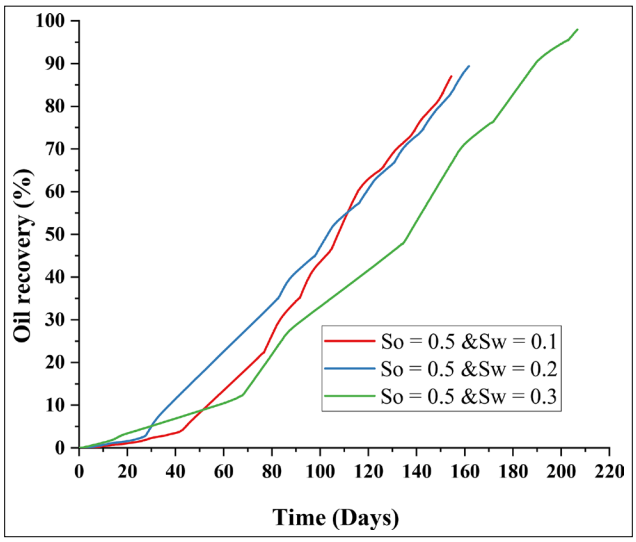

Figure 8: Effect of liquid saturation on oil recovery

Figure 8 shows the effect of initial water saturation on cumulative oil recovery. Cumulative oil recovery is the volumetric oil recovery expressed as a percentage of OOIP. It is evident from **Figure 8** that the oil recovered increased from about 87% to 98% when the water saturation was increased from 10% to 30% because of the increased mobility of heavy oil. Further, the additional water drive created by the increased initial water saturation mobilises the heavy oil towards the production well, resulting in earlier production rates. Hence the time taken to achieve the same amount of recovery was observed to be less in case of increased water saturation when compared to increased oil saturation (**Srinivasa and Suresh, 2014a**).

4. Conclusion

A sensitivity study has been carried out on the initial water saturation in the oil reservoir to understand its effect on the performance of in-situ combustion by using finite difference based numerical tools. The cumulative water recovery was validated to gain confidence in the model concerning the water phase. Initial water saturation of 10%, 20% and 30% was used for the sensitivity study. From the numerical study, it can be concluded that:

- The initial water saturation, which is a measure of OWIP significantly, affects the oil saturation, thermal front and oil production rate;
- A maximum reservoir temperature of about 860 K is observed for a maximum liquid saturation (60% oil saturation and 30% water saturation);
- Cumulative heavy oil recoveries expressed as a percent of OOIP are observed to increase by about 5-7% for a 10% increase in initial water saturation.

A significant increase in average peak temperature of about 160 K (700 K to 860 K) is observed when the water saturation increases from 10% to 30%, with an oil saturation of 60% confirming the effect of water saturation on thermal profiles.

Acknowledgement

The authors gratefully acknowledge research support from the Indian Institute of Technology–Madras and University of Petroleum & Energy Studies.

5. References

Ado, M. R. (2020): Simulation study on the effect of reservoir bottom water on the performance of the THAI in-situ combustion technology for heavy oil/tar sand upgrading and recovery. SN Applied Sciences. 2, 29.

Ahmed, T., Meehan D.N. (2012): Introduction to Enhanced Oil Recovery. Advanced Reservoir Management and Engineering. 2, 541-85.

Aleksandrov, D., and Hascakir, B. (2015): Laboratory Screening tests on the effect of initial oil saturation for the dynamic control of in-situ combustion. Fuel Processing Technology, 130, 224-234.

Bealessio, B.A., Alonso, N.A.B., Mendes, N.J., Sande, A.V., Hascakir, B. (2021): A review of enhanced oil recovery (EOR) methods applied in Kazakhstan, Petroleum, 7, 1, 1-9.

Bueno, N., Mejia, J.M. (2022): Numerical verification of in-situ heavy oil upgrading experiments and thermal processes for enhanced recovery. Fuel. 313. 122730.

Coats, K. H. (1980): In-situ combustion model. Society of Petroleum Engineers Journal, 20, 533-554.

Crookston, R.B., Culham, W. E., and Chen, W. H. (1979): A Numerical simulation model for thermal recovery processes. Society of Petroleum Engineers Journal, 19, 37-58.

Grabowski, J.W., Vinsome, P.K., Lin, R.C., Behie, G.A., and Rubin, B. (1979): A fully implicit general-purpose finite-difference thermal model for in situ combustion and steam. SPE-8396-MS, presented at SPE Annual Technical Conference and Exhibition, Las Vegas, Nevada, 23-26.

Greaves, M., Young, T.J., El-Usta, S., Rathbone, R.R., Ren S.R., and Xia, T.X. (2000): Air injection into light and medium heavy oil reservoirs: Combustion tube studies on west of Shetlands Clair oil and light Australian oil. Chemical Engineering Research and Design, 78, 721-730.

Han, Y., Li, K., and Jia, L. (2021): Modeling Study on Reviving Abandoned Oil Reservoirs by In Situ Combustion Without CO_2 Production While Recovering Both Oil and Heat. ASME *Journal of Energy Resource Technology.* 143, 8, 082902.

He, H., Liu, P., Li, Q., Tang, J., Guan, W., Chen, Y. (2022): Experiments and simulations on factors affecting the stereoscopic fire flooding in heavy oil reservoirs, Fuel, 314, 123-146.

Kavetski, D., Binning, P. and Sloan, S.W., (2001): Adaptive time stepping and error control in a mass conservative numerical solution of the mixed form of Richards equation. Advances in water resources, 24, 6, 595-605.

Kristensen M.R., Gerritsen, M., Thomsen P.G, Michelsen, M.L., and Stenby, E.H. (2007): Efficient integration of stiff kinetics with phase change detection for reactive reservoir processes. Transport in Porous Media, 69, 383-409.

Lin, C.Y., Chen, W.H., Lee, S.T., and Culham, W.E. (1984): Numerical simulation of combustion tube experiments and the associated kinetics of in-situ combustion process. SPE Journal, 24, 657–666.

Meyer, R.F., Attanasi, E.D., and Freeman, P.A. (2007): Heavy oil and natural bitumen resources in geological basins of the world. U.S. Geological Survey, Report 2007–1084.

Nesterov, I.A., Shapiro, A.A., and Stenby, E.H. (2007): Numerical analysis of a one-dimensional multi-component model of the In-situ Combustion process. Journal of Petroleum Science and Engineering, 106, 46-61.

Peaceman, D.W. (1997): Fundamentals of numerical reservoir simulation, Elsevier, 176.

Press, W.H., Teukolsky, S.A., Vellerling, W.T., and Flannery, B.P. (1992): Numerical Recipes in Fortran: The art of scientific computing. Cambridge University Press 2nd edition, 382 p.

Rubin, B., and Buchanan, W.L. (1985): A general purpose thermal model. Society of Petroleum Engineers Journal, 25, 202-214.

Rubin, B., and Vinsome, P.K.W. (1980): The simulation of the in-situ combustion in one dimension using highly implicit finite-difference scheme. Journal of Canadian Petroleum Technology, 19, 68–76.

Sanjeet, S., Pooja, B., Nav, B. (2022): A Study on Nexus Between Renewable Energy and Fossil Fuel Consumption in Commercial Sectors of United States Using Wavelet Coherence and Quantile-on-Quantile Regression. Frontiers in Energy Research, 10.

Sarathi, P.S. (1999): In-situ combustion handbook- principles and practices. Report: DOE/PC/91008-0374.

Srinivasa Reddy, D., and Suresh Kumar, G. (2014a): A Comprehensive analysis on thermal and kinetic aspects of in-situ combustion: Numerical Approach. Applied Mechanics and Material, 592-594, 1393-1397.

Srinivasa Reddy, D., and Suresh Kumar, G. (2014b). A Numerical investigation on role of heavy oil saturation on performance of in-situ combustion in porous media. International Journal of Scientific and Engineering Research, 5, 5, 531-538.

Srinivasareddy, D., and Suresh Kumar, G. (2015): A numerical study on phase behavior effects in enhanced oil recovery by in-situ combustion. Petroleum Science and Technology, 33, 3, 359-363.

Srinivasa Reddy, D., and Suresh Kumar, G. (2015): Numerical simulation of heavy crude oil in porous combustion-tube. Combustion Science and Technology, 187, 12, 1905-1921.

Suresh Kumar, G., and Srinivasa Reddy, D. (2017): Numerical Modeling of Forward In-Situ Combustion Process in Heavy Oil Reservoirs. International Journal of Oil Gas and Coal Technology, 16, 1, 43-57.

Thomas, R.M. and Gladwell, I., (1988): Variable-order variable-step algorithms for second-order systems. Part 1: The methods. International Journal for Numerical Methods in Engineering, 26, 1, 39-53.

Wang, Y., Liu, H., Zhang, Q., Chen, Z., Wang, J., Dong, X., Chen, F. (2020): Pore-scale experimental study on EOR mechanisms of combining thermal and chemical flooding in heavy oil reservoirs, Journal of Petroleum Science and Engineering, 185,106649.

Wood, W. (1990): Practical time-stepping schemes. Oxford University Press, 384 p.

Xu, Q., Long, W., Jiang, H., Zan, C., Huang, J., Chen, X., Shi, L. (2018): Pore-scale modelling of the coupled thermal and reactive flow at the combustion front during crude oil in-situ combustion. Chemical Engineering Journal, 350, 776-790.

Yang, X., and Gates, I.D. (2009): Combustion kinetics of Athabasca bitumen from 1D combustion tube experiments. Natural Resources Research, 18, 193–211.

Yuan, S., Jiang, H., Shi, Y., Ren, Z., Wang, J., Zhang, Y. (2019): Study on heavy oil components transformation path based on core analysis during in-situ combustion process, Fuel, 253, 72-78.

Zheng, H., Shi, W., Ding, D., and Zhang, C. (2017): Numerical Simulation of In Situ Combustion of Oil Shale. Geo Fluids, 1-9.

SAŽETAK

Komparativna analiza utjecaja zasićenja vodom na izgaranje nafte u ležištu

Količina nafte zajedno s ukupnim rezervama vode (engl. *originally in place*, OIP) čini tekuću fazu ležišta teške nafte. Ova količina tekućine prisutna u porama ležišta poznata je kao zasićenje tekućom fazom, a ima vitalnu ulogu u povećanju iscrpka nafte pomoću procesa izgaranja nafte u ležištu (engl. *in situ combustion*, ISC). Naftna faza djeluje kao gorivo i stvara toplinsku energiju potrebnu za smanjenje viskoznosti, a vodena faza potiče stvaranje proširene kondenzacijske zone, koja doprinosi većoj mobilnosti nisko viskozne nafte. Provedeno je numeričko istraživanje utjecaja zasićenja vodom na *in situ* izgaranje u ležištu teške nafte. U sklopu istraživanja razvijen je i vrednovan numerički model za iscrpak vode temeljen na metodi konačnih razlika. Model je korišten za provođenje utjecaja zasićenja tekućinom na izvedbu ISC-a, s obzirom na to da ima vitalnu ulogu u odabiru kriterija za odabir odgovarajućega ISC-a. Dobiveni numerički rezultati upućuju na znatan učinak na toplinski i proizvodni profil tijekom procesa. Usporedba učinka varijacija u zasićenosti vodom i naftom pokazuje znatno povećanje temperature ležišta s povećanjem zasićenosti vodom u odnosu na vodu u slučaju povećanja zasićenosti naftom. Najviše temperature ležišta opažene su pri maksimalnoj zasićenosti tekućinom (nafta i voda zajedno). Nadalje, uočen je dodatni vodonaporni (hidraulični) režim, koji se, zbog povećanja zasićenosti vodom, javlja u ranoj fazi proizvodnje.

Ključne riječi:
povećanje iscrpka nafte, toplinski, zasićenje, *in situ* izgaranje, numeričko modeliranje

Author's Contribution

Tummuri Naga Venkata Pavan (Research Scholar) - conceptualization, formal analysis, and writing. **Srinivasa Reddy Devarapu** (Assistant Professor) - writing, and formal analysis. **Suresh Kumar Govindarajan** (Full Professor) - conceptualization, formal analysis, and manuscript final correction.